

Phase Error Bounds of Fiber Gyro with Polarization-Holding Fiber

WILLIAM K. BURNS, MEMBER, IEEE

Abstract—Phase error bounds for a fiber gyro with an imperfect polarizer are calculated assuming a broad-band source and high-birefringence fiber. The phase error and resulting zero-point drift is related to the polarization-holding parameter h of the fiber. Comparison of the theory with recent experimentally observed bias drift is made.

I. INTRODUCTION

THE RELATIONSHIP between the performance of a fiber-optic gyroscope, the quality of a polarizer used as a polarization filter in the gyro circuit, and the quality of the fiber used in the gyro coil is a topic of current interest. Kintner [1] pointed out that an imperfect polarizer results in a gyro phase bias offset which is proportional to the polarizer amplitude extinction ratio. This phase bias offset also depends on the details of polarization mode coupling in the fiber. A formalism has been developed [2] for the bias offset in a fiber gyro with high-birefringence fiber and a broad-band source, but as only one mode coupling center is assumed, the result is not quantitative. Fredricks and Ulrich [3] have recently estimated an error bound for the phase bias offset for gyros with ordinary low-birefringence fiber, by assuming that a maximum of polarization mode conversion occurs. To date, no one has attempted to treat the intermediate case, where a polarization-holding fiber with small, but finite mode coupling is used. However, the theory to describe such mode coupling in polarization-holding fiber is available, as Kamirow [4] has described polarization mode coupling by random distributions of perturbations, and Rashleigh *et al.*, [5] have provided experimental verification using broad-band sources. In this paper we use an approximate approach to combine the theory of polarization-holding in a high-birefringence fiber with a gyro model for phase bias offset due to an imperfect polarizer and polarization mode coupling, for a gyro with a broad-band source. In particular, we calculate the phase error bounds for a gyro with a broad-band source and high-birefringent fiber. This analysis provides, for the first time, a direct connection between gyro performance and the polarization holding ability of the fiber.

II. THEORY

As noted above, the effect of an imperfect polarizer in a fiber gyro with a broad-band source and a high-birefrin-

gent fiber coil with one-mode coupling center has been analyzed in [2]. The essential result of this calculation was that only if the mode coupling center was located within a depolarization length of the ends or the middle of the fiber coil could it contribute to a phase bias offset in the gyro output. This result is a direct consequence of the low coherence of the broad-band source, and the large group delay difference between the polarization modes of the high-birefringence fiber. The depolarization length [6] is the distance over which light traveling in the two polarization modes loses coherence due to the group delay effect. This result implies that, as far as the phase bias offset is concerned, we can simply ignore mode coupling outside the coherent contributions at the ends and middle of the coil. Mode coupling at other locations will transfer power between the polarization modes, but we can assume this power transfer to be small for reasonable polarization holding fibers.

In a real high-birefringent fiber, mode coupling centers of unknown strength are distributed along the fiber at random positions, so that a detailed description of distributed mode coupling is unrealistic. However, the statistics of the distributed mode coupling is such that it can be described by a single parameter h , where $1/h$ is characteristic of the fiber length over which the modes become coupled. For input power I on the x axis the fraction of power coupled to the y axis after a length L is

$$\frac{\langle I_y \rangle}{I} = \frac{1}{2} [1 - \exp(-2hL)] \quad (1)$$

where $\langle \rangle$ can denote an ensemble average over fiber samples [4] or, for the case of interest here, a spectral average over the bandwidth [5]. With a broad-band source, h can be obtained from a measurement on a single fiber, as each depolarization length L_y provides a statistically independent measure of the coupled power in the length L_y , and a fiber of length L provides $N = L/L_y$ such measurements. It follows then that L_y is the minimum length over which polarization mode coupling can be characterized by the broad-band theory, and that the fraction of power coupled over the length L_y is, on the average, hL_y , where we assume $hL_y \ll 1$.

With this result, we can define the coupled power in a depolarization length in terms of the h parameter of the fiber. In light of the coherence argument given above, this result would seem to be what we need to extend the single-

Manuscript received January 3, 1985; revised June 18, 1985.

The author is with the Naval Research Laboratory, Washington, DC 20375.

IEEE Log Number 8405773.

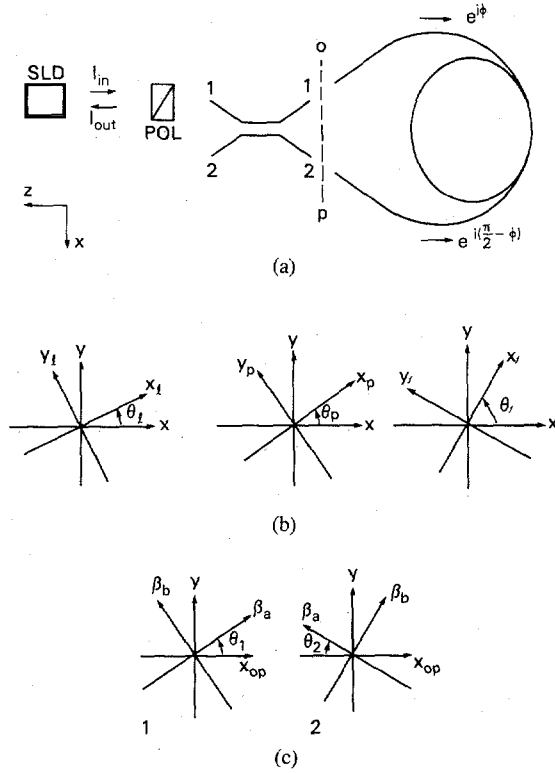


Fig. 1. (a) Fiber gyro configuration assumed in the calculations. (b) Orientation of the source, polarizer, and fiber coupler lead. (c) Orientation of the fiber-coil ends.

coupling center model to a high-birefringent fiber by treating the depolarization lengths at the ends and middle of the fiber coil as lumped elements with mode coupling hL_{γ} . However, to be rigorous, we ought to see if allowing the simultaneous presence of multiple-mode coupling centers introduces additional contributions to the phase bias offset of the same order of magnitude as that calculated in [2]. For this purpose, we will calculate the phase bias offset due to the simultaneous presence of two discrete mode coupling centers, and then consider a fiber with distributed mode coupling.

We will first outline the calculation for the phase bias offset in a gyro with a fiber coil characterized by an arbitrary transfer matrix S , leaving the details to Appendix I. This calculation closely follows that of [2].

We consider a gyroscope arrangement, shown in Fig. 1(a), consisting of a superluminescent diode (SLD) with an arbitrary degree of polarization, an imperfect polarizer, a fiber coupler, and a fiber coil. The gyro signal is taken as that intensity of light returning to the source through the polarizer. The 2×2 directional coupler is assumed to be fabricated from high-birefringence fiber such that it provides 3 dB of coupling for each polarization mode. The fiber comprising the coil is assumed to have linear high-birefringence with resulting difference in mode propagation constant $\Delta\beta = \beta_b - \beta_a$ and length L . The Sagnac phase shift is 2ϕ and we assume an additional non-reciprocal phase shift of $\pi/2$ for propagation in the counter-clockwise direction, to give output equations with maximum sensitivity at zero-rotation rate. In Fig. 1(a),

the fiber coil lies in the X - Z plane and the Y axis is normal to the figure. In Fig. 1(b), we define coordinate axes (X_l, Y_l) , (X_p, Y_p) , and (X_f, Y_f) , and corresponding orientation angles θ_l , θ_p , and θ_f relative to the X - Y frame to define the orientation of the SLD source, polarizer transmission axis, and fiber birefringence axes of the coupler input, respectively. The orientation of the birefringence axes a and b at the fiber-coil ends 1 and 2 are defined in Fig. 1(c) by the orientation angles θ_1 and θ_2 . The birefringence axes undergo a reflection about the Y - Z plane as the loop is traversed. Thus, with our convention in Fig. 1(c), we have $\theta_1 = \theta_2$ for an untwisted fiber. For a loop with axes aligned with the axes of the coupler fiber, as is desirable, we require $\theta_1 = \theta_f$ and $\theta_2 = -\theta_f$. We assume this to be the case.

For a broad-band source with an arbitrary degree of polarization, the time-dependent output may be expressed as

$$\begin{bmatrix} E_{xl}(t) \\ E_{yl}(t) \end{bmatrix} = \begin{bmatrix} ae_{xl}(t) \\ be_{yl}(t) \end{bmatrix} e^{i\omega_0 t} \quad (2)$$

where ω_0 is the source center frequency and we have

$$\langle e_{xl}(t) e_{yl}^*(t) \rangle = \langle e_{yl}(t) e_{xl}^*(t) \rangle = 0 \quad (3)$$

where $\langle \rangle$ signifies time average. Equation (3) expresses the fact that in a partially polarized source there exist axes along which orthogonal field components are uncorrelated. For example, in an SLD, these axes are parallel and perpendicular to the junction plane. The source degree of polarization is defined

$$P = |(2a^2 - 1)| \quad (4)$$

where normalization to unity input requires $a^2 + b^2 = 1$.

To describe the source in a rotated coordinate frame we introduce the rotation matrix

$$C(\theta) = \begin{bmatrix} \cos \theta & -\sin \theta \\ \sin \theta & \cos \theta \end{bmatrix} \quad (5)$$

where θ is the angle between frames. The source field in the polarizer coordinate system is then given by

$$\begin{bmatrix} E_{xp} \\ E_{yp} \end{bmatrix} = C(\theta_{lp}) \begin{bmatrix} E_{xl} \\ E_{yl} \end{bmatrix} \quad (6)$$

where $\theta_{lp} = \theta_l - \theta_p$. Transmission in our imperfect polarizer is defined by

$$\begin{bmatrix} E_{xp} \\ E_{yp} \end{bmatrix}_{\text{trans}} = \begin{bmatrix} 1 & 0 \\ 0 & \epsilon \end{bmatrix} \begin{bmatrix} E_{xp} \\ E_{yp} \end{bmatrix}_{\text{inc}} \quad (7)$$

where X_p is the transmission axis and ϵ is the amplitude extinction coefficient. We assume ϵ small compared to 1. The transmitted source field incident on the birefringent

fiber coupler, in its coordinate frame, is then

$$\begin{bmatrix} E_{xf} \\ E_{yf} \end{bmatrix} = C(\theta_{pf}) \begin{bmatrix} E_{xp} \\ E_{yp} \end{bmatrix}_{\text{trans}} \quad (8)$$

where $\theta_{pf} = \theta_p - \theta_f$.

The coupler transfer matrix is defined by

$$\begin{bmatrix} E_1 \\ E_2 \end{bmatrix}_{\text{out}} = \frac{1}{\sqrt{2}} \begin{bmatrix} 1 & -i \\ -i & 1 \end{bmatrix} \begin{bmatrix} E_1 \\ E_2 \end{bmatrix}_{\text{in}} \quad (9)$$

for both polarizations and in either direction. The subscripts 1 and 2 refer to the coupler leads as shown in Fig. 1(a). We assume the orientations of the birefringent fibers in the coupler are identical and are maintained throughout the coupler. These equations define the time-dependent input fields to the fiber loop.

Propagation in the fiber is governed by the frequency dependent propagation constants $\beta_a = \beta_a(\omega)$ and $\beta_b = \beta_b(\omega)$. We define the transfer matrix of the fiber loop by [10]

$$S_{12} = e^{i\bar{\beta}L} \begin{bmatrix} S_{aa} & S_{ab} \\ -S_{ab}^* & S_{aa}^* \end{bmatrix} \quad (10)$$

where $\bar{\beta} = (\beta_a + \beta_b)/2$ and S_{12} denotes propagation from end 1 to end 2. For propagation from 2 to 1, S_{21} is the inverse of S_{12} . The frequency dependent fiber transfer equations are

$$\begin{bmatrix} E_{a2}^o(\omega) \\ E_{b2}^o(\omega) \end{bmatrix} = e^{i\phi} S_{12} \begin{bmatrix} E_{a1}(\omega) \\ E_{b1}(\omega) \end{bmatrix} \quad (11a)$$

$$\begin{bmatrix} E_{a1}^o(\omega) \\ E_{b1}^o(\omega) \end{bmatrix} = ie^{-i\phi} S_{21} \begin{bmatrix} E_{a2}(\omega) \\ E_{b2}(\omega) \end{bmatrix} \quad (11b)$$

where superscript o denotes an output field. The output fields must be taken back through the coupler, rotated to the polarizer frame, and passed through the polarizer. We require the time-averaged output intensity, to first order in ϵ . The result (see Appendix I) for the gyro signal returned to the source can be expressed for a monochromatic source and a general matrix S as

$$I_p \approx \frac{a^2}{2} [1 + \sin(2\phi + \phi_\epsilon)] \quad (12a)$$

where the phase error ϕ_ϵ is

$$\begin{aligned} \phi_\epsilon \approx & \frac{\epsilon P \tan \theta_{lp}}{a^2} 2 \operatorname{Im}(S_{ab}) [\operatorname{Re}(S_{aa}) \cos 2\theta_{pf} \\ & + \operatorname{Re}(S_{ab}) \sin 2\theta_{pf}]. \end{aligned} \quad (12b)$$

In (12) we refer to the real and imaginary parts of the elements of S and we have assumed $\theta_l \approx \theta_p$, i.e., θ_{lp} is

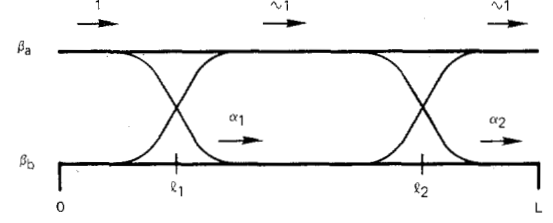


Fig. 2. Model for two mode coupling centers which couple power α_1 and α_2 , respectively, between the polarization modes.

small. We will see that (12b) is a useful representation of ϕ_ϵ due to its generality even though it is a monochromatic result. To calculate (12) for a broad-band source, one must express the time varying fields in terms of a complex analytic signal and follow through the calculation. This has been done explicitly in several references, for example [7]–[9], and implicitly in [2]. This calculation is laborious and, as it involves frequency integrals over the elements of S , does not lead to a concise result. For our purposes, we can obtain the quasimonochromatic result by substituting the elements of S into (12) and then replacing terms of the form $\sin(\Delta\beta z + \phi)$ by terms of the form $\gamma(z) \sin(\Delta\beta_0 z + \phi)$, where $\Delta\beta_0 \equiv \Delta\beta(\omega_0)$ and $\gamma(z)$ is the degree of coherence. $\gamma(z)$ is given by [7]

$$\gamma(z) = \exp \left[- \left(\frac{\delta\omega \delta\tau_g z}{2\sqrt{\ln 2}} \right)^2 \right] \quad (13)$$

for a source with a Gaussian bandshape. In (13), $\delta\omega$ is the half-width at half intensity of the Gaussian spectrum, and $\delta\tau_g = d\Delta\beta/d\omega$ is the fiber group delay difference. The depolarization length L_γ is then the length at which $\gamma(z)$ decays to e^{-1} and is

$$L_\gamma = \frac{2\sqrt{\ln 2}}{\delta\omega \delta\tau_g}. \quad (14)$$

A. Case of Two Mode Coupling Centers

In the fiber loop we assume polarization mode coupling centers which couple fractions of power α_1, α_2 with phases ϕ_1, ϕ_2 between the modes at locations l_1, l_2 , measured from fiber end 1 (Fig. 2). We assume no mode coupling at other points along the fiber. The transfer matrix for the mode coupling center at l_1 , for propagation from $1 \rightarrow 2$ may be expressed

$$\begin{bmatrix} E_a(l_1^+) \\ E_b(l_1^+) \end{bmatrix} = \begin{bmatrix} 1 & \sqrt{\alpha_1} e^{-i\phi_1} \\ -\sqrt{\alpha_1} e^{-i\phi_1} & 1 \end{bmatrix} \begin{bmatrix} E_a(l_1^-) \\ E_b(l_1^-) \end{bmatrix} \quad (15)$$

where l_1^+ and l_1^- refers to just after and just before the coupling center at l_1 , respectively. We assume $\alpha_1 \ll 1$ and neglect the power lost to the input mode. For propagation from $2 \rightarrow 1$, the inverse of the matrix in (15) must be employed. Using (15) and a similar representative for the center at l_2 , the elements of the matrix S are derived

as

$$S_{aa} = e^{\frac{i\Delta\beta L}{2}} - \sqrt{\alpha_1} \sqrt{\alpha_2} \cdot e^{\frac{i\Delta\beta}{2}[L - 2(l_2 - l_1)]} e^{-i(\phi_1 - \phi_2)} \quad (16a)$$

$$S_{ab} = \sqrt{\alpha_1} e^{i\phi_1} e^{i(\Delta\beta/2)(L - 2l_1)} + \sqrt{\alpha_2} e^{i\phi_2} e^{i(\Delta\beta/2)(L - 2l_2)} \quad (16b)$$

Substituting in (12b) yields the coefficients of $\cos 2\theta_{pf}$ and $\sin 2\theta_{pf}$ as

$$\begin{aligned} 2 \operatorname{Im}(S_{ab}) \operatorname{Re}(S_{aa}) = & \sqrt{\alpha_1} \{ \gamma(L - l_1) \cdot \sin[\Delta\beta_0(L - l_1) + \phi_1] - \gamma(l_1) \cdot \sin(\Delta\beta_0 l_1 - \phi_1) \} \\ & + \sqrt{\alpha_2} \{ \gamma(L - l_2) \cdot \sin[\Delta\beta_0(L - l_2) + \phi_2] - \gamma(l_2) \cdot \sin(\Delta\beta_0 l_2 - \phi_2) \} \\ & - \alpha_1 \sqrt{\alpha_2} \gamma(l_2 - 2l_1) \cdot \sin[\Delta\beta_0(l_2 - 2l_1) + 2\phi - \phi] \\ & - \alpha_2 \sqrt{\alpha_1} \gamma(L + l_1 - 2l_2) \cdot \sin[\Delta\beta_0(L + l_1 - 2l_2) + 2\phi_2 - \phi_1] \end{aligned} \quad (17a)$$

$$\begin{aligned} 2 \operatorname{Im}(S_{ab}) \operatorname{Re}(S_{ab}) = & \alpha_1 \gamma(L - 2l_1) \cdot \sin[\Delta\beta_0(L - 2l_1) + 2\phi_1] \\ & + \alpha_2 \gamma(L - 2l_2) \cdot \sin[\Delta\beta_0(L - 2l_2) + 2\phi_2] \\ & + 2\sqrt{\alpha_1} \sqrt{\alpha_2} \gamma(L - l_1 - l_2) \cdot \sin[\Delta\beta_0(L - l_1 - l_2) + \phi_1 + \phi_2] \end{aligned} \quad (17b)$$

where we have inserted the coherence functions as discussed above. Since we assume α small, we expect terms proportional to α , at the fiber center, will be small compared to terms proportional to $\sqrt{\alpha}$, at the fiber ends. The mixed terms, proportional to $\alpha_i \sqrt{\alpha_j}$ or $\sqrt{\alpha_i} \sqrt{\alpha_j}$, are somewhat different in that they can be nonzero for more than two points along the fiber. They must be evaluated by summing over the fiber length. This is done in Appendix II. Finally, we expect alignment so that θ_{pf} is small. Then the terms proportional to $\sin 2\theta_{pf}$ (all of (17b)) can be neglected.

B. Case of Distributed Centers

Now we are in a position to consider a real high-birefringent fiber characterized by the parameter h . We consider first the contributions from scattering centers within

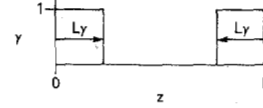


Fig. 3. Model for coherence function versus fiber length for the case of distributed centers.

a depolarization length of the ends of the fiber coil (the first two terms of (17a)). The off-diagonal component S_{ab} of the fiber transfer matrix sums the field components with their proper phase, due to mode coupling along the fiber (16b). In a depolarization length of high-birefringent fiber, this coupled field at the end of the section may be expressed $\sqrt{hL_\gamma} e^{i\phi}$, where the phase ϕ is unknown. To approximately account for coherent effects we construct a model as shown in Fig. 3. We include coupling centers within L_γ of each end of the fiber by assuming a coherence function $\gamma = 1$ over each of those regions. We take $\gamma = 0$ over the rest of the fiber and, assuming $hL \ll 1$, neglect the power transfer that occurs due to mode coupling over the fiber. The transfer matrix for the depolarization length is given by [10]

$$S(L_\gamma) = e^{-i\beta L_\gamma} \begin{bmatrix} e^{i(\Delta\beta/2)L_\gamma} & \sqrt{hL_\gamma} e^{i\phi} \\ -\sqrt{hL_\gamma} e^{-i\phi} & e^{-i(\Delta\beta/2)L_\gamma} \end{bmatrix} \quad (18)$$

We are assuming that the coupled power is sufficiently small that it doesn't perturb the phase of the uncoupled power. Using (18) at each end of the fiber and a propagation matrix from $z = L_\gamma$ to $z = L - L_\gamma$, we obtain the fiber transfer matrix for propagation from $1 \rightarrow 2$, which has coefficients

$$S_{aa} = e^{i(\Delta\beta/2)L} \quad (19a)$$

$$S_{ab} = \sqrt{hL_\gamma} [e^{i\phi_1} e^{i(\Delta\beta/2)(L - L_\gamma)} + e^{i\phi_2} e^{-i(\Delta\beta/2)(L - L_\gamma)}] \quad (19b)$$

ϕ_1 and ϕ_2 are the additional phases due to mode coupling at the ends of the fiber. In general, $\phi_1 \neq \phi_2$ since the random distributions of coupling centers are different at each end of the fiber. However, we take the magnitude of the coupled power for each distribution to be approximated by the mean value hL_γ . Finally, we substitute (19) into (12b) to obtain the phase error ϕ_ϵ

$$\phi_\epsilon = \frac{\epsilon P \tan \theta_{lp}}{a^2} \sqrt{hL_\gamma} \cdot \left[\sin \left(\phi_1 - \frac{\Delta\beta L_\gamma}{2} \right) + \sin \left(\phi_2 + \frac{\Delta\beta L_\gamma}{2} \right) \right] \quad (20)$$

where we have taken $\cos 2\theta_{pf} = 1$ and dropped the two nonphysical sine terms that are displayed in (17a). In a rigorous derivation, these two terms would have zero coherence function coefficients. As the sine functions can

TABLE I
COMPARISON OF CALCULATED AND OBSERVED BIAS DRIFT

gyro	$\lambda(\text{\AA})$	$L_y(\text{cm})$	ϵ^2	P	$\theta_{LP}(\text{deg})$	$ \phi_{\epsilon} _{\text{max}}(\text{deg/hr})$	Observed bias drift (deg/hr)
bulk component (Ref. 11)	95	7.0	10^{-5}	0.4	10	0.017	0.035 (24 hr)
all fiber (Ref. 12)	40	16.5	10^{-3}	0.2	10	0.15	0.25 (215 hr)

have arbitrary arguments, the upper bound on ϕ_{ϵ} is

$$|\phi_{\epsilon}| \leq \frac{2\epsilon P \theta_{LP} \sqrt{hL_y}}{a^2} \quad (21)$$

for small θ_{LP} .

In Appendix II we consider the magnitude of the terms involving multiple coupling centers in (17), and show that they are all small compared to the first order term in (21). Equation (21) should then represent a valid upper bound for the phase bias offset.

III. DISCUSSION

Equation (21) demonstrates the advantage of the use of broad-band sources and high-birefringent fiber in fiber-optic gyroscopes. It is interesting to compare our result with the low-birefringence result of [3]. For low-birefringence fiber, the quantity hL_y approaches 1/2 over the fiber length, and the factor $2\sqrt{hL_y}$ in (21) would become $1/\sqrt{2}$. The phase bias error is then reduced by a factor $2\sqrt{2}hL_y$ for the high-birefringence case. Assuming typical values of $h \sim 10^{-6} \text{ m}^{-1}$, and $L_y \sim 10^{-1} \text{ m}$, this factor is $\sim 10^{-3}$.

We also can compare the calculated phase error from (21) with recent experimental results for bias drift in gyros with high-birefringent fiber. Results from two experiments are available: one with bulk and fiber components [11] and one in an all-fiber configuration [12]. The fiber coil used was identical in each case. Fiber length was 430 m on a 16-cm radius and the wavelength was $0.8 \mu\text{m}$, giving a scale factor for both gyros of $5.7 \cdot 10^4 \text{ }^\circ/\text{h/rad}$. The high-birefringent fiber was made by Hitachi and had a measured h of 3.10^{-6} m^{-1} and group delay difference [13] ($\delta\tau_g$) of 0.9 ns/km . The relevant experimental parameters for each case are given in Table I with L_y calculated from (14). The experimentally observed bias drift at zero rotation rate is shown along with the period of time the observation was made. In each case the error bound calculated for ϕ_{ϵ} is within a factor of two of the peak-to-peak bias drift observed. However, we don't know if the phase of the polarization mode coupled power is stable during the course of the experiments, or if it varies through 2π or some lesser amount. Thus, we don't know if the mode coupling which is responsible for the phase error calculated here was the physical mechanism which caused the experimental bias drift. All we can conclude is that the calculated magnitude of the mode coupling effect makes

it a candidate for causing at least part of the experimental bias drift.

In conclusion, we have used an approximate model to relate the fiber gyro phase error due to polarization mode coupling in the fiber to the polarization-holding parameter of the fiber. Comparison of the theoretical result with current experiments indicates that this effect may be sufficiently large to play a role in observed bias drift. The theoretical result should allow fiber gyro designers to specify the required fiber and polarizer quality necessary for a given gyro performance.

APPENDIX I

Starting from (9), the outputs of the fiber coupler are

$$\begin{bmatrix} E_{xf} \\ E_{yf} \end{bmatrix}_{\text{out},1} = \frac{1}{\sqrt{2}} \begin{bmatrix} E_{xf} \\ E_{yf} \end{bmatrix}_{\text{in}} \quad (\text{A1a})$$

$$\begin{bmatrix} E_{xf} \\ E_{yf} \end{bmatrix}_{\text{out},2} = \frac{-i}{\sqrt{2}} \begin{bmatrix} E_{xf} \\ E_{yf} \end{bmatrix}_{\text{in}} \quad (\text{A1b})$$

in terms of the input to the fiber lead (see (8)). The inputs to the fiber coil, for the assumed axis alignment are

$$\begin{bmatrix} E_{a1} \\ E_{b1} \end{bmatrix} = \begin{bmatrix} E_{xf} \\ E_{yf} \end{bmatrix}_{\text{out},1} \quad (\text{A2a})$$

$$\begin{bmatrix} E_{a2} \\ E_{b2} \end{bmatrix} = \begin{bmatrix} -E_{xf} \\ E_{yf} \end{bmatrix}_{\text{out},2} \quad (\text{A2b})$$

Using (11), the outputs of the fiber coil are

$$\begin{bmatrix} E_{a2}^o \\ E_{b2}^o \end{bmatrix} = \frac{e^{i\phi} e^{-i\beta L}}{\sqrt{2}} S_{12} \begin{bmatrix} E_{xf} \\ E_{yf} \end{bmatrix}_{\text{in}} \quad (\text{A3a})$$

$$\begin{bmatrix} E_{a1}^o \\ E_{b1}^o \end{bmatrix} = \frac{e^{-i\phi} e^{-i\beta L}}{\sqrt{2}} S_{21} \begin{bmatrix} -E_{xf} \\ E_{yf} \end{bmatrix}_{\text{in}} \quad (\text{A3b})$$

Then, using (A2), the fields input to the fiber coupler are

$$\begin{bmatrix} E_{xf} \\ E_{yf} \end{bmatrix}_1 = \frac{e^{-i\phi} e^{-i\beta L}}{\sqrt{2}} \begin{bmatrix} -S_{aa} & -S_{ab}^* \\ -S_{ab} & S_{aa}^* \end{bmatrix} \begin{bmatrix} E_{xf} \\ E_{yf} \end{bmatrix}_{\text{in}} \quad (\text{A4a})$$

$$\begin{bmatrix} E_{xf} \\ E_{yf} \end{bmatrix}_2 = \frac{e^{i\phi} e^{-i\beta L}}{\sqrt{2}} \begin{bmatrix} -S_{aa} & -S_{ab} \\ -S_{ab}^* & S_{aa}^* \end{bmatrix} \begin{bmatrix} E_{xf} \\ E_{yf} \end{bmatrix}_{\text{in}} \quad (\text{A4b})$$

Finally, using (9), the output of the fiber coupled lead is

related to the input to that lead by

$$\begin{bmatrix} E_{xf}^o \\ E_{yf}^o \end{bmatrix}_1 = \frac{1}{2} e^{-i\beta L} \begin{bmatrix} -(e^{-i\phi} - ie^{i\phi}) S_{aa} & -e^{-i\phi} S_{ab}^* + ie^{i\phi} S_{ab} \\ -e^{-i\phi} S_{ab} + ie^{i\phi} S_{ab}^* & (e^{-i\phi} - ie^{i\phi}) S_{aa}^* \end{bmatrix} \begin{bmatrix} E_{xf} \\ E_{yf} \end{bmatrix}_{in} \quad (A5)$$

where the superscript o denotes an output field. The output field in the polarizer frame is

$$\begin{bmatrix} E_{xp}^o \\ E_{yp}^o \end{bmatrix} = C(-\theta_{pf}) \begin{bmatrix} E_{xf}^o \\ E_{yf}^o \end{bmatrix}_1 \quad (A6)$$

and the output intensity through the polarizer is

$$I_p = \langle |E_{xp}^o(t)|^2 \rangle \quad (A7)$$

to first order in ϵ . Again, ignoring the quasi-monochromatic aspect of the problem, the output intensity through the polarizer, in terms of the input intensity on the polarizer (6), becomes

$$\begin{aligned} \langle |E_{xp}^o|^2 \rangle &\approx \frac{1}{2} \{ \langle |E_{xp}|^2 \rangle (1 + \sin 2\phi) \\ &+ 2\epsilon \langle |E_{xp}| |E_{yp}| \rangle \text{Im}(S_{ab}) \cos 2\phi \\ &\cdot [\text{Re}(S_{aa}) \cos 2\theta_{pf} + \text{Re}(S_{ab}) \sin 2\theta_{pf}] \} \end{aligned} \quad (A8)$$

where we have dropped terms which do not affect the phase bias offset. Equation (A8) may be recast as

$$I_p \approx \frac{1}{2} \langle |E_{xp}|^2 \rangle [1 + \sin(2\phi + \phi_\epsilon)] \quad (A9a)$$

$$\begin{aligned} \phi_\epsilon &\approx 2\epsilon \frac{\langle |E_{xp}| |E_{yp}| \rangle}{\langle |E_{xp}|^2 \rangle} \text{Im}(S_{ab}) [\text{Re}(S_{aa}) \cos 2\theta_{pf} \\ &+ \text{Re}(S_{ab}) \sin 2\theta_{pf}] \end{aligned} \quad (A9b)$$

where from (2), (3), and (6)

$$\langle |E_{xp}|^2 \rangle = a^2 \cos^2 \theta_{lp} + b^2 \sin^2 \theta_{lp} \approx a^2 \quad (A10a)$$

$$\frac{\langle |E_{xp}| |E_{yp}| \rangle}{\langle |E_{xp}|^2 \rangle} = \frac{(a^2 - b^2) \sin \theta_{lp} \cos \theta_{lp}}{a^2 \cos^2 \theta_{lp} + b^2 \sin^2 \theta_{lp}} \approx \frac{P \tan \theta_{lp}}{a^2} \quad (A10b)$$

for small θ_{lp} . Substituting (A10) into (A9) yields (12).

APPENDIX II

Here we will consider the magnitude of the third and fourth terms of (17a) and the third term of (17b). We take

first the third term of (17a). This term is nonzero for all sets of mode coupling centers within depolarization lengths centered at l_1 and l_2 such that $l_2 = 2l_1$. Each contribution is of the form $\alpha_1 \sqrt{\alpha_2} \sin(2\phi_1 - \phi_2)$ with ϕ_1 and ϕ_2 arbitrary. For depolarization length L_γ we expect $N = L/L_\gamma$ contributions as l_2 varies from 0 to L . Omitting proportionality terms, we have

$$\phi_\epsilon \sim (hL_\gamma)^{3/2} \sum_{i=1}^N [\sin(2\phi_1 - \phi_2)]_i \quad (A11)$$

where we have taken $\alpha_1 \approx \alpha_2 \approx hL_\gamma$. Since ϕ_1 and ϕ_2 vary arbitrarily, we approximate each contribution by $\pm(\sin)_{\text{ave}}$, where the average value of the sine is $2/\pi$. The summation can then be treated as a random walk problem, and the sum evaluates to $\sqrt{N(2/\pi)}$. We have

$$\phi_\epsilon \sim (hL_\gamma)^{3/2} \sqrt{N} \frac{2}{\pi} = \frac{2hL_\gamma}{\pi} \sqrt{hL}. \quad (A12)$$

For typical values, $h \sim 10^{-6}/m$, $L \sim 10^3$, $L_\gamma \sim 10^{-1} m$, this contribution is small compared to $2\sqrt{hL_\gamma}$ in (21). The contribution from the fourth term in (17a) is identical to the third so both may be neglected. For the third term of (17b) nonzero contributions are obtained for sets of mode coupling centers within depolarization lengths at l_1 and l_2 such that $l_1 + l_2 = L$. There are $N = L/2L_\gamma$ such contributions. We obtain for $\alpha_1 \approx \alpha_2 \approx hL_\gamma$

$$\phi_\epsilon \sim 2hL_\gamma \sqrt{N} \frac{2}{\pi} = \frac{2h}{\pi} \sqrt{2L_\gamma L} \quad (A13)$$

which is also small compared to $2\sqrt{hL_\gamma}$ for the values quoted above. Finally, we conclude that considerations of three or more mode coupling centers will bring in additional higher-order terms which will also be small compared to the first-order term in (21).

ACKNOWLEDGMENT

The author acknowledges helpful discussions on this problem with C. L. Chen, and the receipt of some of the experimental parameters from R. P. Moeller.

REFERENCES

- [1] E. C. Kintner, "Polarization control in optical-fiber gyroscopes," *Opt. Lett.*, vol. 6, p. 154, 1981.
- [2] W. K. Burns and R. P. Moeller, "Polarizer requirements for fiber gyroscopes with high birefringence fiber and broad-band sources," *J. Lightwave Technol.*, vol. LT-2, p. 430, 1984.
- [3] R. J. Fredricks, and R. Ulrich, "Phase error bounds of fiber gyro with imperfect polariser/depolariser," *Electron. Lett.*, vol. 20, p. 330, 1984.
- [4] I. P. Kaminow, "Polarization in optical fibers," *IEEE J. Quantum Electron.*, vol. QE-17, p. 15, 1981.
- [5] S. C. Rashleigh, W. K. Burns, R. P. Moeller, and R. Ulrich, "Polarization holding in birefringent single-mode fibers," *Opt. Lett.*, vol. 7, p. 40, 1982.
- [6] S. C. Rashleigh and R. Ulrich, "Polarization mode dispersion in single-mode fibers," *Opt. Lett.*, vol. 3, 1978.
- [7] J. I. Sakai, S. Machida, and T. Kimura, "Degree of polarization in

anisotropic single-mode optical fibers: theory," *IEEE J. Quantum Electron.*, vol. QE-18, p. 488, 1982.

- [8] W. K. Burns, C. L. Chen, and R. P. Moeller, "Fiber-optic gyroscopes with broad-band sources," *J. Lightwave Technol.*, vol. LT-1, p. 98, 1983.
- [9] W. K. Burns, "Degree of polarization in the Lyot depolarizer," *J. Lightwave Technol.*, vol. LT-1, p. 475, 1983.
- [10] G. A. Pavlath and H. J. Shaw, "Birefringence and polarization effects in fiber gyroscopes," *Appl. Opt.*, vol. 21, p. 1752, 1982.
- [11] W. K. Burns, R. P. Moeller, C. A. Villarruel, and M. Abebe, "Fiber-optic gyroscope with polarization-holding fiber," *Opt. Lett.*, vol. 8, p. 540, 1983.
- [12] W. K. Burns, R. P. Moeller, C. A. Villarruel, and M. Abebe, "All-fiber gyroscope with polarization-holding fiber," *Opt. Lett.*, vol. 9, p. 570, 1984.
- [13] W. K. Burns and R. P. Moeller, "Measurement of polarization mode dispersion in high-birefringence fiber," *Opt. Lett.*, vol. 8, p. 195, 1983.



William K. Burns (M'80) was born in Philadelphia, PA, in June 1943. He received the B.S. degree in engineering physics from Cornell University, Ithaca, NY, in 1965, and the M.S. and Ph.D. degrees in applied physics from Harvard University, Cambridge, MA, in 1967 and 1971, respectively. His thesis research was in nonlinear optics.

During 1971 he was a staff member at Arthur D. Little, Inc., Cambridge, MA, where he contributed to various laser-related studies and surveys. Since 1972 he has been a Research Physicist at the Naval Research Laboratory, Washington, DC. He is presently Head of the Optical Waveguide Section of the Optical Techniques Branch. His research interests include integrated optics, single-mode fiber optics, and the application of single-mode technology to communications, sensors, and signal processing.

Dr. Burns is a member of the Optical Society of America.